

**Military Technical College
Kobry El-kobbah,
Cairo, Egypt**



**5th International Confer
on Electrical Engineer**

ICEENG 2006

THE EFFECT OF IMPERFECT SYMBOL TIMING ESTIMATION ON THE PERFORMANCE OF SPACE-TIME CODED SYSTEMS

Hazem Abu Elhassan Radi, Yahya Z. Mohasseb, and Ali Elmogazy

ABSTRACT

This paper addresses the effects of errors in symbol timing estimation on the performance of space time coded systems. Fixed and uniformly distributed timing errors with different variances are assumed. Furthermore, the improvement of timing estimates with increase in signal to noise ratio is modeled to yield practical expectations of performance. This symbol timing-error is applied to a simple transmit diversity scheme using QPSK, 8PSK modulations. This paper could be useful guide for definition of requirement in symbol timing systems used in space time coding systems.

I. INTRODUCTION

Multiple-antenna wireless systems have received considerable attention over the past several years as it can offer substantial performance improvement to a wireless communication system by providing spatial diversity and supporting high data rate services. These systems can provide significantly higher capacity as compared with single-antenna systems without requiring an increase in system bandwidth [1]. Capacity of single antenna systems increase with the logarithm of SNR. Multiple antenna systems classically employ multiple antennas at the receiver, forming a receiver diversity system. Such a system increases capacity with the log of the number of receive antennas and mitigates multipath fading. [2],[3], Emre Telatar & Foschini calculate the capacity of Multiple-Input Multiple-Output (MIMO) antenna systems. A means to achieve near capacity results were demonstrated in [4]. In which it was shown that, MIMO systems have an extraordinary high spectral efficiency and support large fade level reduction due to exploitation rather than mitigation of multipath effects. Furthermore it achieves co-channel interference reduction. In [5], a simple transmit diversity scheme was proposed, these space-time codes (STCs) achieve significant error rate improvements over single-antenna error-correcting codes. Space-Time-Coding (STC) is a method of transmitting multiple data beams on multiple transmitters to multiple receivers. There are two main types of STCs, namely space-time block codes (STBC) and space-time trellis codes (STTC). Space-time block codes operate on a block of input symbols, producing a matrix output whose columns represent time and rows represent antennas. On the other hand, space-time trellis codes operate on one input symbol at a time, producing a sequence vector symbols whose length represents antennas. The original scheme of (STC) was based on trellis codes but the simpler block codes were utilized by Alamouti in [6]. Later Tarokh et al. in [7], [8] developed space-time block-codes (STBCs).

For simplicity, previous proposed papers, for both space-time block coding (STBC) and space-time trellis coding (STTC) schemes, assumed known or perfect estimated symbol

Deleted: achieve the expected performance gain as in

timing to evaluate the performance [6], [9]. Timing estimation errors between the transmit and received signals could degrade the system performance. This paper focuses on illustrating the effect of imperfect symbol timing estimation on the performance of Alamouti's space-time-coding MIMO transmission model. The results are presented for two antenna system.

Deleted: ,

Symbol timing recovery is critical for reliable data detection in modern digital communications, the continuous-time received signal is sampled and these samples are used to make the decisions on the transmitted symbols. The receiver has to know the starting and finishing time instants of the individual symbols in order to correctly determine the proper sampling instant. There are a number of techniques to recover the symbol timing. In general they can be categorized as [10], pure analog timing recovery, mixed (analog-digital) timing recovery, and all-digital timing recovery. The first two techniques require voltage control oscillator (VCOs) to create synchronized timing clocks, these techniques are mainly used in conventional receivers, where the symbol synchronization is performed using a feedback loop which controls the phase of the sampling clock. In the third technique the continuous-time received signal is sampled using a fixed oversampling clock that is not synchronized to the incoming symbols. Consequently, timing adjustment must be done by digital methods after sampling. There are two approaches to implement these digital adjustments [11], Data-Aided (DA) timing recovery approach, and Non-Data-Aided (NDA) timing recovery approach.

In data-aided timing recovery systems [12-14], training sequences are transmitted along with the data-bearing signal, in the receiver, these training sequences are oversampled and these samples are used in extracting the symbol timing through different timing recovery algorithms. Such an approach minimizes the time required to synchronize the receiver to the transmitter, and is typically used in mobile communication systems where the channel characteristics are rapidly changing, and the transmission is bursty. However, the training symbols reduce bandwidth and power efficiencies. Furthermore, the epoch of the orthogonal training sequences has to be correctly identified, if errors occur in identifying the epoch, the performance of symbol timing synchronization degrades.

In Non-Data-Aided (NDA) timing recovery [15], [16], the use of training sequences is avoided and the receiver carries out the task of timing extraction using the sampled data-bearing signal. Both throughput and power efficiency are improved but at the expense of an increase in time taken to establish timing synchronization.

Although there is a small loss of performance (increase in timing-error variance for the same SNR) in (DA) approach compared to (NDA) approach, the advantage of the (NDA) approach is that it does not require any training sequences so that transmission efficiency is increased. Furthermore, symbol timing estimation can be performed any time during the transmission and no epoch of training sequences needs to be identified, thereby saving computation power and eliminating the risk of performance degradation due to incorrect identification of training sequences' epoch [15].

Following, Signal Model is given in section II. The performance study of Alamouti space-time-coding transmission systems under the effect of imperfect symbol timing estimation is given in section III, different timing-error patterns are considered (fixed, variable, bounded, diminishing variant timing error). Results are given for two different modulation schemes; QPSK, and 8-ary PSK. Conclusion comes in section IV.

II. SIGNAL MODEL

Deleted: The

The simplified base band equivalent model for G2 Alamouti's space-time coding wireless system is shown in Fig 1.

Consider an information source which generates frames of length L symbols drawn from certain constellation as shown in Fig 1.

$$F = (x_1, x_2, x_3 \dots x_L) \tag{1}$$

Each frame is then space-time encoded. For simplicity we consider a simple two transmitter-based scheme associated with $p = 2$ proposed by Alamouti in [6]. For such encoder, the transmitted symbols are arranged into pairs

$$(x_i, x_{i+1}) \quad \text{where } i=1,3,\dots,L-1 \quad (2)$$

During the j^{th} symbol period, the two symbols are simultaneously transmitted from two different antennas. Then, during the $(j+1)^{\text{th}}$ symbol period, the first antenna transmits $-x_j$ while the second antenna transmits \bar{x}_j where \bar{x} denotes the complex conjugate of x . Thus, the transmitted sequences from the first and the second antennas, denoted Seq_1 & Seq_2 respectively, can be written as

$$Seq_1 = (x_1, -\bar{x}_2, \dots, x_j, -\bar{x}_{j+1}, \dots, -\bar{x}_L) \quad (3)$$

$$Seq_2 = (x_2, \bar{x}_1, \dots, x_{j+1}, \bar{x}_j, \dots, \bar{x}_{L-1}) \quad (4)$$

In [6], the model was derived under assumption of perfect timing information. Therefore, only the outputs of the matched filters were considered and no ISI is modeled. Such a model is inadequate for the purpose of this paper. Thus, we rederive the continuous time model, taking the pulse shape into consideration. The model presented in [6] becomes a special case obtained at the correct sampling instant. Thus, each stream of encoded symbols is independently pulse-shaped and transmitted from the corresponding antenna, $i=1, 2$

$$S_i(t) = \sqrt{E_s} \sum_{l=1}^L Seq_i(l) p(t - lT_s) \quad (5)$$

Where $T_s = 1/R_s$ is the symbol period, and $p(t)$ is the transmit filter pulse shaping function. Without loss of generality, assume that $p(t)$ is a square root raised-cosine pulse shape

$$p(t) = \frac{4\varepsilon}{\pi\sqrt{T_s}} \cdot \frac{\cos((1+\varepsilon)\pi/T_s) + \frac{\sin((1+\varepsilon)\pi/T_s)}{(4\varepsilon/T_s)}}{(4\varepsilon/T_s)^2 - 1} \quad (6)$$

where ε is the bandwidth expansion or roll-off factor, $p(t)$ is truncated to $\pm 3T_s$ around $t=0$. The two signals, $s_1(t)$ and $s_2(t)$ produced from the pulse-shaping are transmitted simultaneously from the two transmitters, namely, Tx₁ and Tx₂.

The fading channel coefficients among various transmitters and receivers are denoted $h_{ji}(t)$, where $h_{ji}(t)$ is the channel impulse response (CIR) between the receiver j , and transmitter i . $h_{ji}(t)$ is modeled by a complex random variable with Rayleigh distributed amplitude and uniform phase. Moreover we assume that the coherence time of the channel is larger than the $2T_s$, so that the channel does not change over the period of transmission of x_{j+1} . Therefore, it can be written as

$$h_{ji}((2l-1)T_s) = h_{ji}(2lT_s) \quad (7)$$

where $l = 1, 2 \dots L/2$, $L =$ the frame length

Fig. 1 shows the block diagram of a mobile receiver equipped with two receive antennas. The received signal at the j^{th} receiver can be modeled as

$$r_j(t) = \sum_{i=1}^2 h_{ji}(t) s_i(t) + n_j(t) \quad (8)$$

where $n_j(t) =$ time varying additive white Gaussian noise at receiver j .

Substituting from (5) then,

$$r_j(t) = \sqrt{E_s} \sum_{i=1}^2 h_{ji}(t) \sum_{l=1}^L Seq_i(l) p(t - lT_s) + n_j(t) \quad (9)$$

The output of the matched filter is

$$y_j(t) = \sqrt{E_s} \sum_{i=1}^2 h_{ji}(t) \sum_{l=1}^L x_i(l) \rho(t-lT_s) + \bar{n}_j(t) \quad (10)$$

Where $\rho(t) = p(t) * p(t)$ is the autocorrelation function of the square root raised cosine pulse shape, and $\bar{n}_j(t) = n_j(t) * p(t)$ is the colored noise.

The receiver is assumed to employ an all-digital timing recovery mechanism. Thus, the outputs of the matched filters are over sampled with $f_{o.s}$ which is Q times faster than the symbol rate R_s ,

$$f_{o.s} = Q \cdot R_s \quad (11)$$

Then, the time instant of the k^{th} sample within the l^{th} matched filter output symbol, $t_{l,k}$ will be

$$t_{l,k} = lT_s + \frac{k}{Q} T_s + \delta T_s \quad (12)$$

where δT_s is the timing error, $l=1, 2 \dots L$ symbol index, and $k=1, 2 \dots Q$ the sample index. Then, the received samples at the j^{th} antenna matched filter output will be

$$y_j(t_{l,k}) = \sqrt{E_s} \sum_{i=1}^2 h_{ji}(t_{l,k}) \sum_{l=1}^L Seq_i(l) \rho(t_{l,k} - lT_s) + \bar{n}_j(t_{l,k}) \quad (13)$$

These samples are first, used for timing extraction and frequency synchronization using one of the known timing and channel estimation algorithms mentioned above. Then, the samples corresponding to the information symbols, at the optimum sampling instant, with the channel estimation are fed to an ST channel decoder, which consists mainly of a combiner and a maximum likelihood detector.

Optimum sampling instant for symbol l'

$$t_{opt}(l') = l'T_s \quad (14)$$

Then, the j^{th} optimum timing sampled received signals is

$$y_j(t_{opt}) = \sqrt{E_s} \sum_{i=1}^2 h_{ji}(l'T_s) \sum_{l=1}^L Seq_i(l') \rho((l' - l)T_s) + \bar{n}_j(t_{opt}) \quad (15)$$

Considering the properties of the square root raised cosine pulse shape

$$\rho(0) = 1 \quad (16)$$

$$\rho(kT_s) = 0 \quad (17)$$

Then,

$$y_j(l') = \sqrt{E_s} \sum_{i=1}^2 h_{ji}(l'T_s) Seq_i(l') + \bar{n}_j(t_{opt}) \quad (18)$$

Which is the equation used in [6]

At the combiner, the two optimum-timing sampled received signals along with the channel estimation, are combined producing (18), (19)

$$\tilde{y}(2l-1) = \sum_{i=1}^2 (\bar{h}_{i1}(2l-1)y_i(2l-1) + h_{i2}(2l)\bar{y}_i(2l)) \quad (19)$$

$$\tilde{y}(2l) = \sum_{i=1}^2 (\bar{h}_{i2}(2l-1)y_i(2l-1) + h_{i1}(2l)\bar{y}_i(2l)) \quad (20)$$

where $l=1, 2 \dots L/2$

Taking into consideration (7), then

$$\tilde{y}(2l-1) = \sum_{i=1}^2 \left[(|h_{i1}(2l)|^2 + |h_{i2}(2l)|^2) Seq_i(2l-1) + \bar{h}_{i1}n_i(2l-1) + h_{i2}\bar{n}_i(2l) \right] \quad (21)$$

$$\tilde{y}(2l) = \sum_{i=1}^2 \left[(|h_{i1}(2l)|^2 + |h_{i2}(2l)|^2) \text{Seq}_i(2l) + \bar{h}_{i2}n_i(2l-1) - h_{i1}\bar{n}_i(2l) \right] \quad (22)$$

Finally, the combined signal $\tilde{y}(l)$ is fed to the maximum likelihood detector where most likely transmitted symbol is determined based on the minimum Euclidean distance between the combined signal and all possible transmitted symbols.

III. SIMULATION RESULTS

The Alamouti's STBC described in the previous section is simulated under various conditions representing timing errors. The simulation model assumes a root raised cosine pulse shaping with a roll-off factor $\varepsilon=0.3$. Since the timing offsets are in practice drawn from a continuous distribution, an excessive over-sampling with $Q=100$ is used to generate timing error with a resolution of $0.01T_s$. Timing errors are modeled in three different methods. First, the effect of a fixed timing shift is considered. Second, the timing error is assumed to be a random variable with uniform distribution. In practice, timing error variance is reduced due to improvement in its estimation with the increase of SNR. Such improvement is taken into consideration in the third method.

In the first method the effect of fixed error in timing estimation, is carried out by adding different fixed timing offsets Δt to the ideal timing instant (t_{opt}). These timing offsets are set to be a certain percentage of T_s .

In the second method, the timing-error Δt is assumed to be a random variable uniformly distributed between $[-\alpha, +\alpha]$ where $0 \leq \alpha \leq 0.5T_s$. The model adds a bounded random variable timing offset, Δt to the ideal timing instant (t_{opt}). These random timing offsets are set to be bounded by certain percentage of T_s .

In the third method, which is the most realistic case, the timing-error is assumed to be a uniform distributed random variable, having a diminishing variance with increasing SNR. In order to form a diminishing variance characteristic of the timing error, a simulation squaring timing recovery technique-one of the Non-Data-Aided (NDA) timing recovery techniques-is used to determine the appropriate timing-error variances corresponding to different SNR. A simulation model for Squaring Timing Recovery technique was carried out in order to estimate different variances of timing error estimation in accordance to SNR. This simulation was carried out as in [15], using two transmitters and two receivers MIMO system with oversampling ratio =4. Results are given in Fig. 5, 10 which show the dependence of timing error estimation variances on SNR for both QPSK and 8PSK modulation schemes respectively.

Taking into consideration that the variance of a uniform distributed random variable is given by,

$$\text{var}(\Delta t) = \frac{1}{12}(a - b)^2 \quad \text{as } \Delta t \text{ varies over } [a,b] \quad (25)$$

Each SNR is assigned to its corresponding varying time offset boundaries, then the simulation model adds these different-bounded variant timing offsets, Δt to the matched filter output sampling clock in correspondence to SNR.

In each case of modeling the timing error, the results will be compared with the performance under perfect timing recovery. Moreover the results for the power loss will be given for each case.

It is assumed that the timing estimate is calculated and used over a frame length $L=100$ symbols. Hence, each timing error is kept constant over 100 symbols, results are averaged over 10^5 loops. The simulation is carried over SNR range (0 - 26 dB) for QPSK

Deleted: distribution for each frame?.

Deleted: /

Deleted: r

Deleted: e

Deleted: taking into consideration thtaking into consideration th Then, taking into consideration the THEvariance

Deleted: variable IS

Deleted: e

Deleted: Also a

Deleted: study of

modulation scheme and. (0 - 20 dB) for 8PSK modulation scheme, for each value of SNR, random values of the timing error are used to calculate the average BER.

Fig. 2, 3 shows the performance of Alamouti's STBC using QPSK modulation scheme under the effect of fixed, and bounded variant timing error compared with the performance under perfect timing, respectively. Fig. 2 shows the performance under a fixed timing offset $\Delta t = (0.05, 0.1, 0.15, 0.2, 0.25)T_s$. Fig. 3 shows the performance under a random variant uniformly distributed timing offset Δt , which is bounded by $[-\alpha, +\alpha]$, where $\alpha = (0.05, 0.1, 0.15, 0.2, 0.25)T_s$.

It is clear that the performance degrades significantly under both schemes with error increasing in the amount of timing offset, and the major drawback of the imperfect timing estimation is that the performance (BER) suffers from an error floor behavior, which could be overcome with any further increasing in SNR. Fig. 2 shows that these error floors are $10^{-5}, 5 \times 10^{-6}, 6 \times 10^{-5}, 5 \times 10^{-4}$ and 3×10^{-3} for $0.05T_s, 0.1T_s, 0.15T_s, 0.2T_s, 0.25T_s$ fixed timing error respectively. Fig. 2 shows also that fixed timing error results in an excessive amount of power loss in order to achieve certain performance level, for example to achieve $BER=10^{-4}$ $0.05T_s, 0.1T_s$ fixed timing errors cause a power loss equal to 0.9, 2.8 (dB), respectively and equal to 2.5, 6.2 (dB) for $BER=10^{-5}$

Fig. 3 shows that these error floors are $6 \times 10^{-7}, 2 \times 10^{-6}, 9 \times 10^{-6}, 8 \times 10^{-5}$ and 3×10^{-4} $[-5\%, 5\%]T_s, [-10\%, 10\%]T_s, [-15\%, 15\%]T_s, [-20\%, 20\%]T_s,$ and $[-25\%, 25\%]T_s$ bounded variable timing error respectively. Fig. 3 shows also that bounded variable timing error results in an excessive amount of power loss in order to achieve certain performance level, for example to achieve $BER=10^{-4}$, a $[-5\%, 5\%]T_s, [-10\%, 10\%]T_s, [-15\%, 15\%]T_s, [-20\%, 20\%]T_s$ bounded variable timing error cause a power loss equal to 0.7, 1.8, 3 and 10 (dB), respectively.

Fig. 3 also shows that, these timing errors prevent systems from achieving certain performances, for example systems suffer from $[-10\%, 10\%]T_s, [-20\%, 20\%]T_s$ bounded variable timing error are not able to achieve $10^{-6}, 10^{-5}$ respectively, even with any increasing SNR.

Fig. 4 shows the power loss due to bounded timing error. For example it shows that, in order to achieve $BER=10^{-5}$ in a wireless communication employing an Alamouti's STBC using QPSK modulation scheme that suffers from $[-5\%, 5\%]T_s, [-10\%, 10\%]T_s$ bounded variable timing error, an additional SNR = 1.8, 3.6 (dB) must be used, respectively, and the amount increases to be 2.2, 4.2 (dB) at $BER = 5 \times 10^{-6}$

Fig. 5 shows the improvement in timing error estimation (decreasing of timing error variance) with increasing in SNR for Alamouti's STBC using QPSK modulation scheme. Fig. 6 shows the most realistic case, the performance under the effect of diminishing-variable timing – given in Fig. 5 – compared with the performance under perfect timing. It is clear that the two performances are identical for low SNR, as the effect of noise is more dominant, for high SNR the effect of noise vanishes and the effect of imperfect timing estimation degrades the performance significantly.

Fig. 7, 8 shows the performance of Alamouti's STBC using 8PSK modulation scheme under the effect of fixed, and bounded variant timing error compared with the performance under perfect timing, respectively. Fig. 7 shows the performance under a fixed timing offset $\Delta t = (0.05, 0.1, 0.15, 0.2, 0.25)T_s$. Fig. 8 shows the performance under a random variant uniformly distributed timing offset Δt , which is bounded by $[-\alpha, +\alpha]$, where $\alpha = (0.05, 0.1, 0.15, 0.2, 0.25)T_s$.

It is clear that the performance degrades significantly under both schemes with error increasing in the amount of timing offset, and the major drawback of the imperfect timing

estimation is that the performance (BER) suffers from an error floor behavior, which could be overcome with any further increasing in SNR.

Fig. 7 shows that these error floor are 2×10^{-4} , 10^{-3} , 6×10^{-3} , 3×10^{-2} and 7×10^{-2} for $0.05T_s$, $0.1T_s$, $0.15T_s$, $0.2T_s$, $0.25T_s$ fixed timing error respectively. Fig. 7 shows also that fixed timing error results in an excessive amount of power loss in order to achieve certain performance level, for example to achieve $BER=10^{-2}$, a $0.05T_s$, $0.1T_s$ fixed timing error cause a power loss equal to 1.2, 3.9 (dB), respectively and equal to 5, 17.6 (dB) for $BER=10^{-3}$

Fig. 8 shows that these error floor are 3×10^{-4} , 6×10^{-4} , 2×10^{-3} , 6×10^{-3} and 10^{-2} $[-5\%, 5\%]T_s$, $[-10\%, 10\%]T_s$, $[-15\%, 15\%]T_s$, $[-20\%, 20\%]T_s$, and $[-25\%, 25\%]T_s$ bounded variable timing error respectively. Fig. 8 shows also that bounded variable timing error results in an excessive amount of power loss in order to achieve certain performance level, for example to achieve $BER=10^{-2}$, a $[-5\%, 5\%]T_s$, $[-10\%, 10\%]T_s$, $[-15\%, 15\%]T_s$, $[-20\%, 20\%]T_s$ bounded variable timing error cause a power loss equal to 1, 2, 5.6 and 12.5 (dB) respectively. Fig. 8 also shows that, these timing errors prevent systems from achieving certain performances, for example systems suffer from $[-10\%, 10\%]T_s$, $[-20\%, 20\%]T_s$ bounded variable timing error are not able to achieve 10^{-4} , 10^{-3} respectively, even with an increasing in SNR. Fig. 9 shows the power loss due to bounded timing error, which shows that in order to achieve $BER=10^{-3}$ in a wireless communication employing an Alamouti STBC using 8PSK modulation scheme that suffers from $[-5\%, 5\%]T_s$, $[-10\%, 10\%]T_s$ bounded variable timing error, an excessive bit SNR = 1.5, 3.8 (dB) must be used, respectively and this amount increases to be 2.8, 7 (dB) at $BER = 5 \times 10^{-3}$. Fig.10 shows, the improvement in timing error estimation (decreasing of timing error variance) with increasing in SNR. Alamouti's STBC using 8PSK modulation scheme. Fig. 11 shows the most realistic case, performance under the effect of diminishing-variance variant timing – given in Fig. 10 compared with the performance under perfect timing. It is clear that the two performances are identical for low SNR where the effect of noise is more dominant, for high SNR the effect of noise vanishes and the effect of imperfect timing estimation degrades the performance significantly.

IV. CONCLUSIONS

Symbol timing estimation error causes significant degradation in system performance Alamouti's STBC wireless communication systems using both QPSK, and 8PSK modulation schemes. The major drawback of symbol timing estimation errors is that it causes the system performance to suffer from an error floor behavior that prevents the system from achieving certain BER, even with any increasing in SNR. Results in this paper could be a useful guide for definition of requirement in symbol timing systems used in space time coding wireless systems that are designed to achieve certain performance level

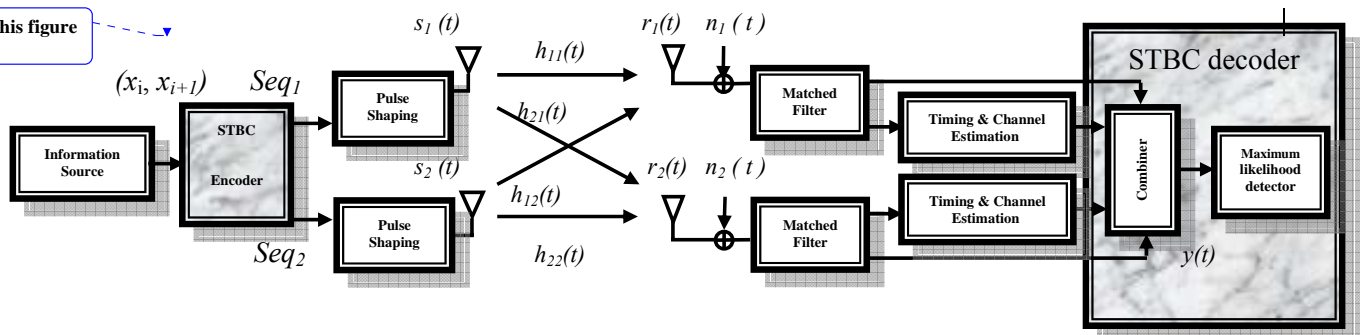


Fig.1. Simplified base band equivalent model for G2 Alamouti's space-time coding wireless system

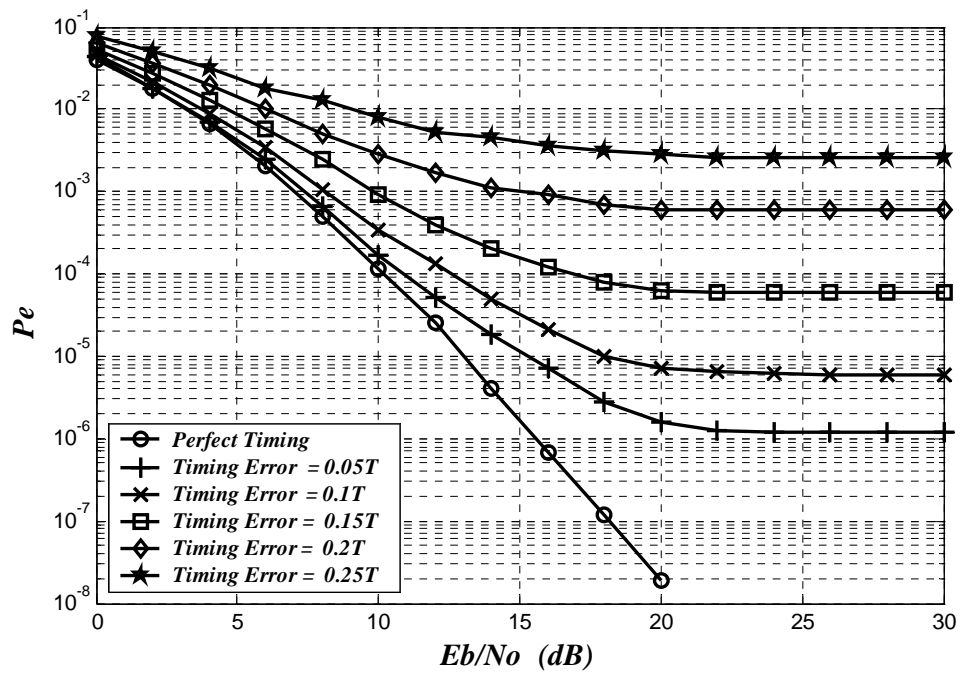


Fig.2 The performance of Alamouti's STBC using QPSK modulation scheme under the effect of different fixed timing error

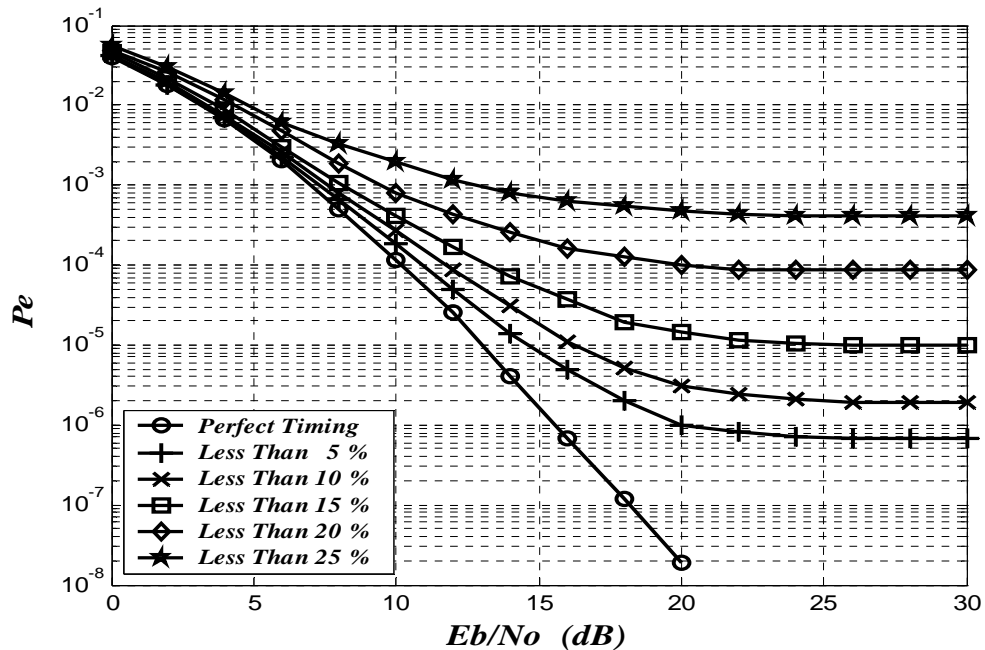


Fig.3 The performance of Alamouti's STBC using QPSK modulation scheme under the effect of different bounded variant timing error

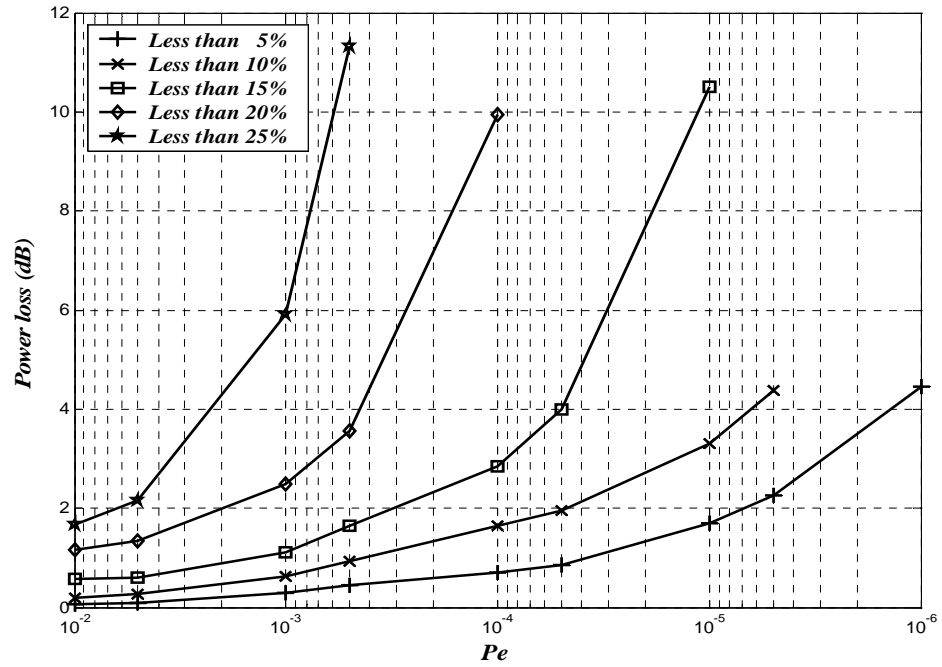


Fig.4 Power losses effect of different bounded variant timing error over Alamouti's STBC using QPSK modulation scheme

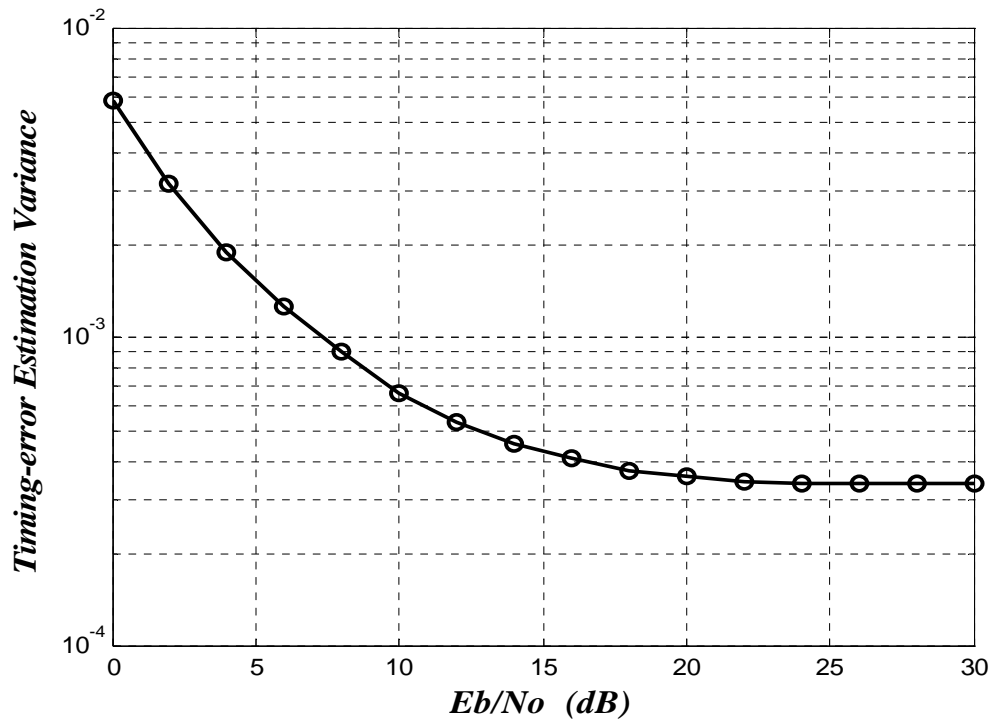


Fig.5 QPSK Timing error estimation diminishing variance

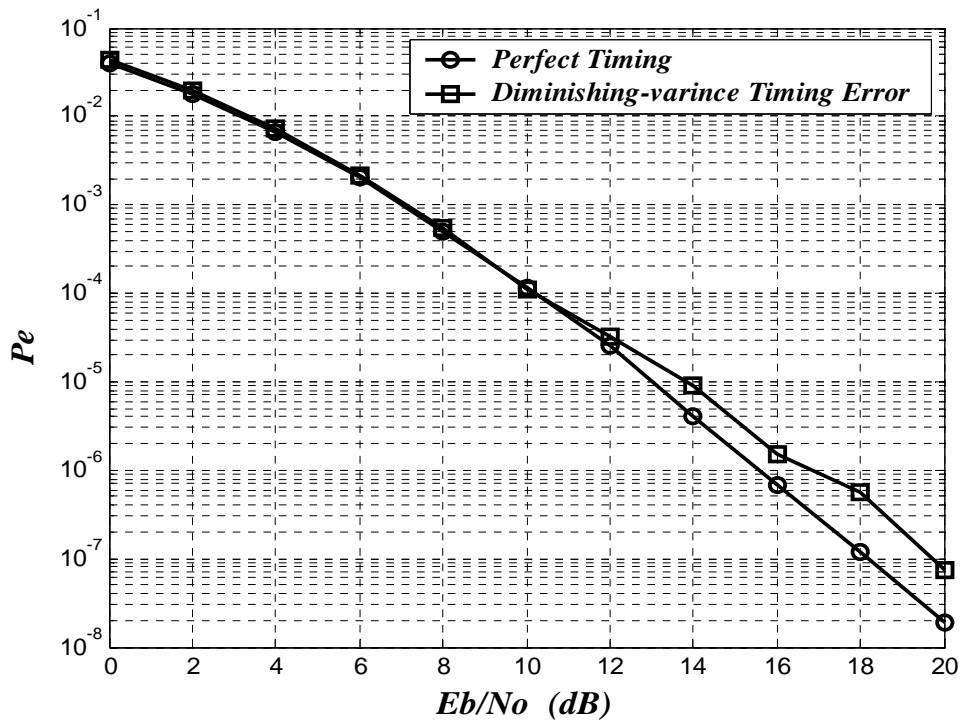


Fig 6 The performance of Alamouti's STBC using QPSK modulation scheme under the effect of a diminishing-variance variant timing error

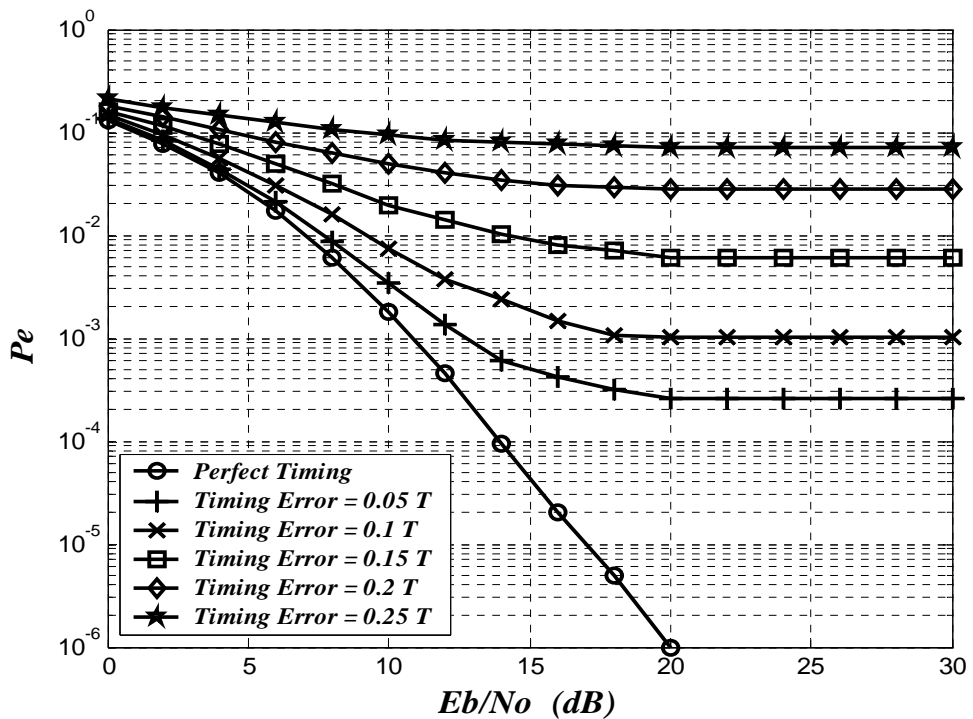


Fig.7 The performance of Alamouti's STBC using 8PSK modulation scheme under the effect of different fixed timing error

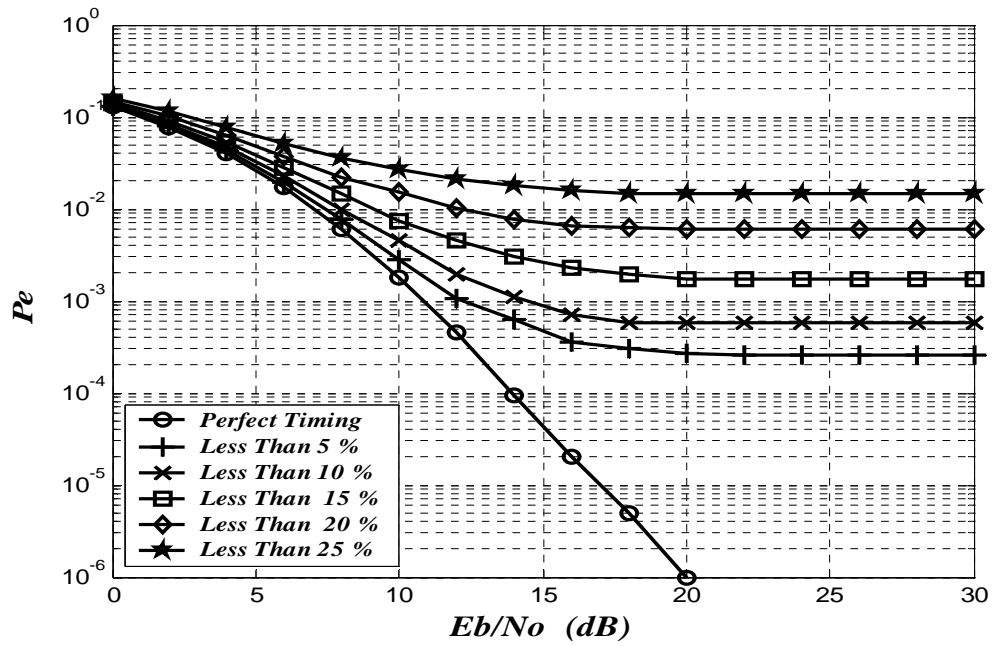


Fig.8 The performance of Alamouti's STBC using 8PSK modulation scheme under the effect of different bounded variant timing error

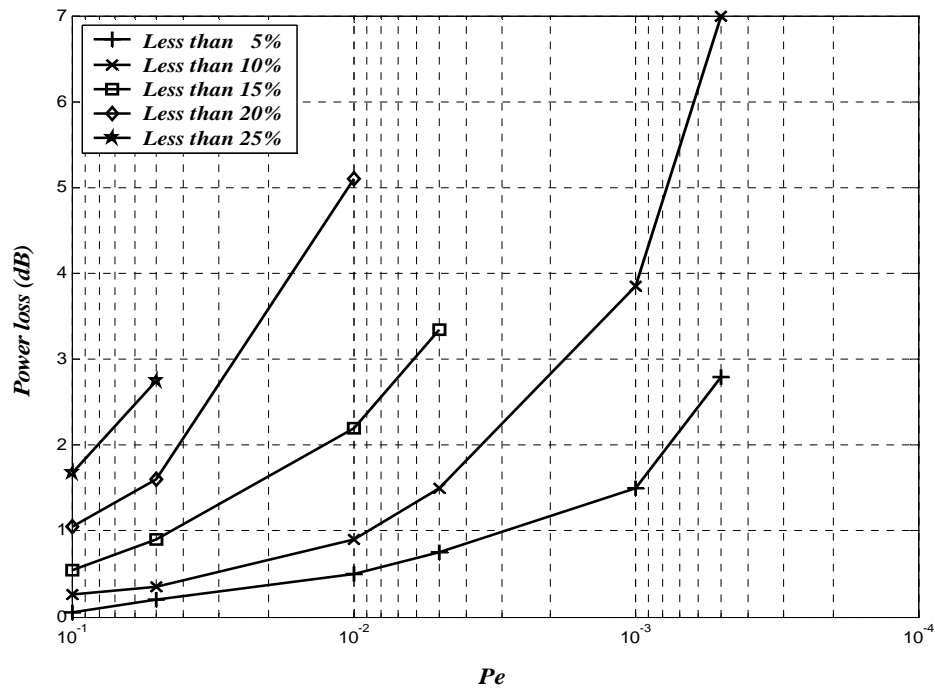


Fig.9 Power losses effect of different bounded variant timing error over Alamouti's STBC using 8PSK modulation scheme

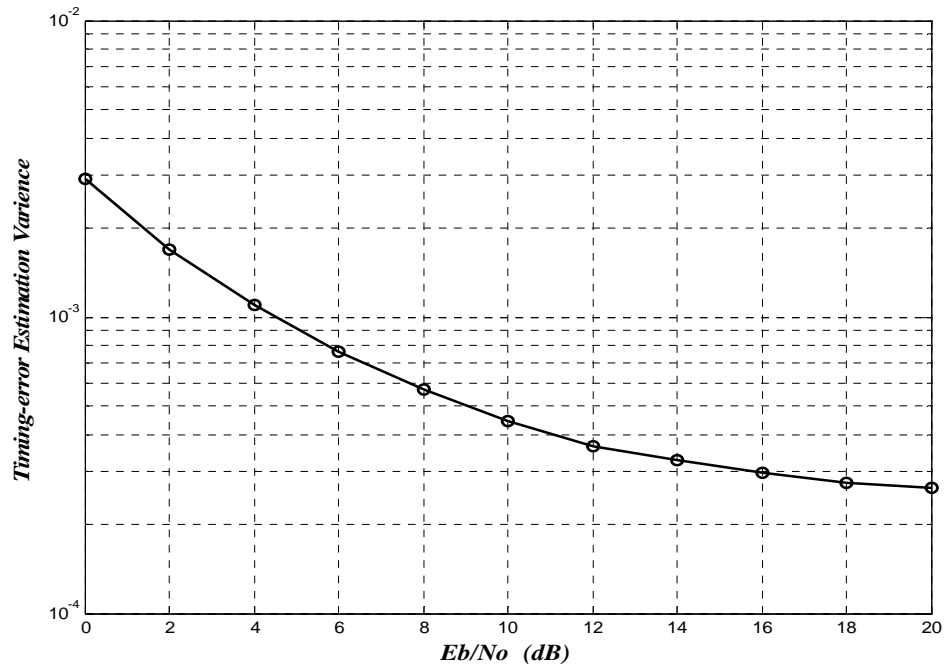


Fig.10 QPSK Timing error estimation diminishing variance

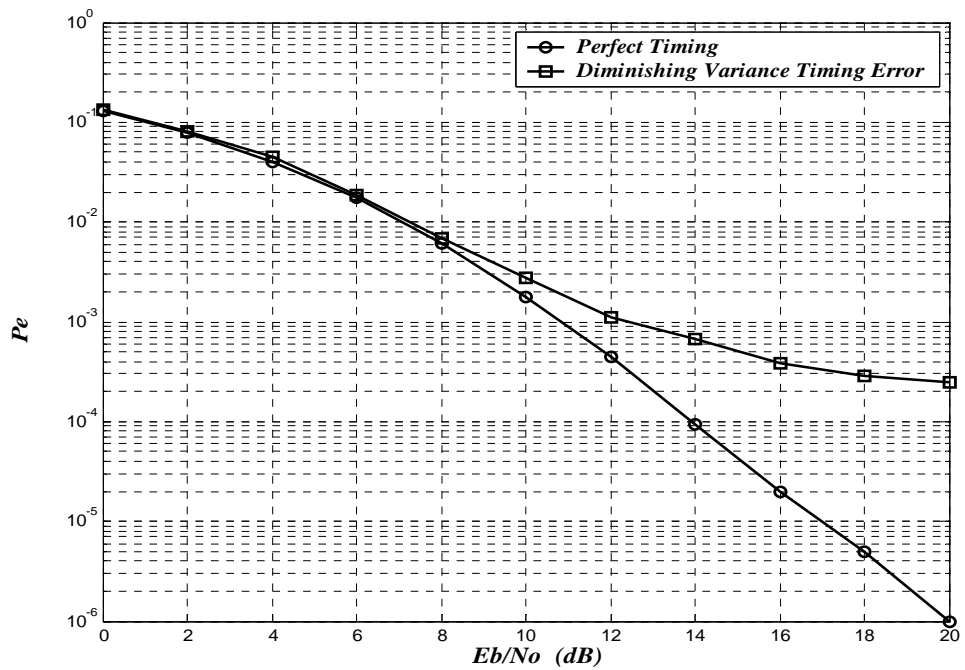


Fig.11 The performance of Alamouti's STBC using 8PSK modulation scheme under the effect a diminishing-variance variant timing error

REFRANCES

- [1] I. E. Telatar, "Capacity of multi-antenna Gaussian channel," Eur. Trans. Telecommu vol.10, pp.585–595, Nov./Dec.1999.
- [2] Emre Telatar (October 1995). "Capacity of multi-antenna gaussian channels". Technical Memorandum, Bell Laboratories.
- [3] G. J. Foschini and M. J. Gans, "On limits of wireless communication in a fading environment when using multiple antennas," Wireless Personal Commun., vol.6, no.3, pp.311–35, Mar.1998.
- [4] G. J. Foschini, "Layered space-time architecture for wireless communication in a fadi environment when using multi-element antennas," Bell Labs. Tech. J., vol.1, no.2, pp.41–. 1996.
- [5] V. Tarokh, N. Seshadri, and A. Calderbank, "Space–time codes for high data rate wirel communication: Performance criterion and code construction," IEEE Trans. Inform. Theo vol.44, pp. 744–765, Mar.1998.
- [6] S. M. Alamouti, "A simple transmit diversity technique for wireless communication IEEE J. Select. Areas in Commun., vol. 16, pp. 1451-1458, Oct. 1998.
- [7] V. Tarokh, H. Jafarkhani and A. R. Calderbank, "Space-time block coding for wirel communications: performance results," IEEE J. Select. Areas in Commun., vol. 17, pp. 4: 460, Mar. 1999.
- [8] V. Tarokh, H. Jafarkhani and A. R. Calderbank, "Space-time block coding for wirel communications: theory of generalized orthogonal designs", IEEE Transactions Information Theory, Vol.45, No.4, pp.1456-1467, July 1999.
- [9] A. F. Naguib, V. Tarokh, N. Seshadri and A. R. Calderbank, "A space-time codi modem for high-data-rate wireless communications," IEEE J. Select. Areas in Commu vol.16, pp.1459-1478, Oct.1998.
- [10] Hong-Kui Yang' and Martin Snelgrove "Symbol Timing Recovery Using Oversamplin Techniques" Communications, 1996. ICC 96, Conference Record, Converging Technologie for Tomorrow's Applications. 1996 IEEE International Conference, Vol. 3, pp.1296 – 1300 Jun. 1996
- [11] S. Haykin, *Communication systems*, John Wiley & Sons, Edition: 4, May. 2000, ISBN: 0471178691
- [12] Y.-C. Wu, S. C. Chan and E. Serpedin, "Symbol-timing estimation in space-time codi systems based on orthogonal training sequences," IEEE Trans. on Wireless Communicatio VOL. 4, NO. 2, Mar. 2005.
- [13] Y.-C. Wu and E. Serpedin, "Symbol Timing Estimation in MIMO Correlated Flat-Fadi Channels," Wireless Communications and Mobile Computing, Special Issue on MIN Communications, Wiley, vol.4, Issue 7, pp.773-790, Nov.2004.
- [14] Y.-C. Wu and E. Serpedin, "Data-aided maximum likelihood symbol timing estimati in MIMO correlated fading channels," Proceedings of IEEE ICASSP 04, vol.4, pp.829-8: May 2004.
- [15] Y.-C. Wu and S.-C. Chan, "On the symbol timing recovery in space-time codi systems," Proceedings of IEEE Wireless Communications and Networking Conferer (WCNC) 2003, pp. 420-424, Mar. 2003.
- [16] Y.-C. Wu and E. Serpedin, "Non-data-aided ML Symbol Timing Estimation in MIMC Correlated Fading Channels," Vehicular Technology Conference, 2005. VTC-2005-Fall. 20 IEEE 62nd, Vol. 4, pp.2091 – 2095, Sept., 2005